Thermodynamics of an integrable model for electrons with correlated hopping

1995 J. Phys. A: Math. Gen. 28 4453

(http://iopscience.iop.org/0305-4470/28/16/006)

J. Phys. A: Math. Gen. 28 (1995) 4453–4468. Printed in the UK

Thermodynamics of an integrable model for electrons with correlated hopping

Gerald Bedürftig† and Holger Frahm‡
Institut für Theoretische Physik, Universität Hannover, D-30167 Hannover, Germany

Received 5 April 1995

Abstract. A new supersymmetric model for electrons with generalized hopping terms and Hubbard interaction on a one-dimensional lattice is solved by means of the Bethe ansatz. We investigate the phase diagram of this model by studying the ground state and excitations of the model as a function of the interaction parameter, electronic density and magnetization. Using arguments from conformal field theory we can study the critical exponents describing the asymptotic behaviour of correlation functions at long distances.

1. Introduction

In recent years, studies of one-dimensional models of electronic systems have been a primary source for gaining an understanding of correlation effects in low-dimensional systems. In particular, the growing number of exactly soluble models such as the Bethe ansatz integrable Hubbard model and supersymmetric t–J models and their extensions have provided new insights into the ground-state properties of these systems [1–5].

Different sources of interaction have been studied in these models: apart from the influence of the on-site Coulomb repulsion (which is the main physical motivation leading to the Hubbard model) and the antiferromagnetic coupling of electrons leading to spin fluctuations (as present in the t–J model) the kinetic energy can been modified to include interaction effects. Such *bond–charge* repulsion terms reflecting the dependence of nearest-neighbour hopping amplitudes on the occupation of sites affected were first discussed in [6]. There have been extensive studies of the relevance of such additional interaction terms, for example in their relation to the possibility of superconductivity based on electronic correlations (see e.g. [7, 8]). Furthermore, several exact solutions for one-dimensional models of this type have been found (see e.g. [4, 5, 9]).

In this paper we consider a new integrable model containing generalized hopping integrals that have recently been found [10, 11]. The Hamiltonian is given as

$$\begin{aligned}\mathcal{H} = -\sum_i \sum_{\sigma=\uparrow\downarrow} \left(c_{i\sigma}^\dagger c_{i+1\sigma} + \mathrm{HC}\right)\left(t_0 - X(n_{i,-\sigma} + n_{i+1,-\sigma}) + \bar{X}, n_{i,-\sigma} n_{i+1,-\sigma}\right) \\ -t_3 \sum_i \left(c_{i+1,\uparrow}^\dagger c_{i+1,\downarrow}^\dagger c_{i\downarrow} c_{i\uparrow} + \mathrm{HC}\right) + U \sum_i n_{i\uparrow} n_{i\downarrow} - \mu \sum_i (n_{i\uparrow} + n_{i\downarrow}) \\ -\frac{h}{2} \sum_i (n_{i\uparrow} - n_{i\downarrow}). \qquad (1.1)\end{aligned}$$

† E-mail: bed@itp.uni-hannover.de
‡ E-mail: frahm@itp.uni-hannover.de

0305-4470/95/164453+16$19.50

In addition to the usual single-particle hopping amplitude t_0 and the on-site Coulomb integral U, it contains the bond–charge interaction X, an additional coupling $\tilde{X}$ correlating hopping amplitudes with the local occupation, and a pair hopping term with amplitude t_3. In addition, the Hamiltonian contains a coupling to a chemical potential μ and magnetic field h, controlling particle density and magnetization of the system respectively.

For later convenience we introduce a different parametrization of the hopping integrals by $X = t_0 - t_1$, $\tilde{X} = t_0 - 2t_1 + t_2$. Studying the two-particle scattering matrix $\mathcal{S}$ one finds two possible choices of the parameters t_j and U where $\mathcal{S}$ satisfies a Yang–Baxter equation resulting in candidates for models (1.1) that might be integrable by means of the Bethe ansatz: first, choosing $t_0 = t_1 = t_2$ (which implies $X = \tilde{X} = 0$) and $t_3 = 0$ the Hamiltonian reduces to the well-known Hubbard model [1]. Another family of such models arises for†

$$\tfrac{1}{2}U = -t_3 = \pm(t_0 - t_2) \neq 0 \qquad (t_1)^2 = t_0 t_2. \tag{1.2}$$

In an independent approach, the integrability of model (1.1) with (1.2) has been proven in the framework of the quantum inverse scattering method where the Hamiltonian has been derived from a solution of the quantum Yang–Baxter equation, invariant under a four-dimensional representation of $gl(2|1)$ [10] which is the symmetry underlying the (Bethe ansatz soluble) supersymmetric t–J model.

Our paper is organized as follows. In the following section we shall discuss the symmetries of the Hamiltonian (1.1) at the integrable point (1.2). It turns out that there are two physically different regions to be studied corresponding to $t_0 > t_2$ and $t_0 < t_2$ (or positive and negative U), respectively. In section 3 the Bethe ansatz equations determining the spectrum of the model are derived. In section 4 ground-state properties and the spectrum of low-lying excitations at temperature $T = 0$ are determined, and in section 5 we shall study finite-size corrections of the spectrum to discuss the asymptotic behaviour of correlation functions. In the appendix we discuss the completeness of the solutions obtained from these equations for small systems.

2. Symmetries

Owing to various symmetries of Hamiltonian (1.1), only the upper sign in relation (1.2) with positive t_0 and t_2 has to be studied. To see this, we first note that the sign of t_1 is not fixed by conditions (1.2). In fact, the unitary transformation

$$c_{i\sigma} \to c_{i\sigma}(1 - 2n_{i,-\sigma}) \tag{2.1}$$

only has the effect of changing $t_1 \to -t_1$.

A particle–hole transformation performs a mapping between $t_0, t_2 > 0$ and $t_0, t_2 < 0$ (as a consequence of (1.2) t_0 and t_2 necessarily have the same sign!):

$$T_1 : c_{i\sigma} \to c_{i\sigma}^{\dagger} \qquad \sigma = \uparrow, \downarrow . \tag{2.2}$$

Applying this transform to the Hamiltonian we obtain (the irrelevant change of sign in t_1 is suppressed)

$$\mathcal{H}(t_0, t_2, U = \pm 2(t_0 - t_2), \mu, h) \longrightarrow \mathcal{H}(-t_2, -t_0, U = \pm 2(t_0 - t_2), \mu', -h) + (\mu' - \mu)L. \tag{2.3}$$

Here $\mu' = 2(t_0 - t_2) - \mu$ and L is the number of lattice sites.

The transformation

$$T_2 : c_{i\sigma} \to (-1)^i c_{i\sigma} \qquad \sigma = \uparrow, \downarrow \tag{2.4}$$

† The special cases $t_2 = t_0/2$ and $t_2 = 2t_0$ have already been discussed in [12].

changes the sign of the single-particle dispersion resulting in

$$\mathcal{H}(t_0, t_2, U = \pm 2(t_0 - t_2), \mu, h) \to \mathcal{H}(-t_0, -t_2, U = \pm 2(t_0 - t_2), \mu, h). \tag{2.5}$$

Applying both T_1 and T_2 the sign in the first equation of (1.2) is reversed (see figure 1):

$$\mathcal{H}(t_0, t_2, U = \pm 2(t_0 - t_2), \mu, h) \longrightarrow \mathcal{H}(t_2, t_0, U = \mp 2(t_2 - t_0), \mu', -h) + (\mu' - \mu)L. \tag{2.6}$$

Hence, t_2 and t_0 are interchanged and at the same time the electronic density is changed from n_e to $2 - n_e$. As will be seen later the Bethe ansatz solution in the region $t_0, t_2 > 0$ extends throughout the interval $0 \leqslant n_e < 2$. Hence it is sufficient to consider the model with $U = +2(t_0 - t_2)$ in this region.

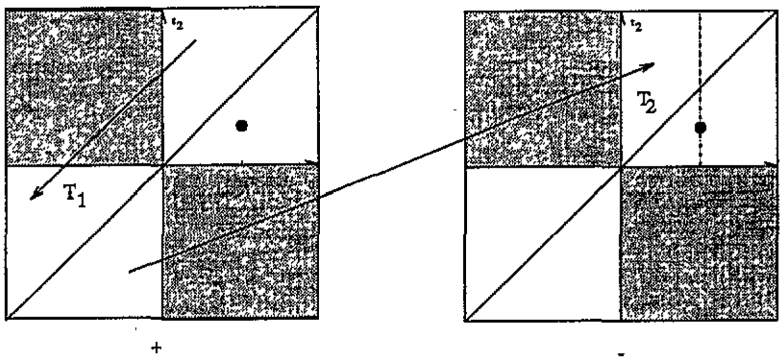

Figure 1. Range of parameters t_0, t_2 for which model (1.1) is integrable as a consequence of (1.2) for $U = +2(t_0 - t_2)$ (left) and $U = -2(t_0 - t_2)$ (right). The dots mark the model introduced in [12].

As already mentioned, the model can be constructed in the framework of the quantum inverse scattering method based on an irreducible representation of the algebra $gl(2|1)$. This is reflected in additional invariances of the Hamiltonian: apart from the $SU(2)$ spin and number operator

$$S^z = \frac{1}{2}\sum_{i=1}^{L}(n_{i\downarrow} - n_{i\uparrow}) \qquad S^+ = \sum_{i=1}^{L} c_{i,\uparrow}^\dagger c_{i,\downarrow} \qquad S^- = \left(S^+\right)^\dagger \qquad N_e = \sum_{i=1}^{L}(n_{i\uparrow} + n_{i\downarrow}) \tag{2.7}$$

which commute with the Hamiltonian for vanishing magnetic field, there are four additional supersymmetric generators [10], namely

$$Q_\sigma = \sum_{i=1}^{L}(-1)^i c_{i,\sigma}\left(\frac{t_1}{t_0}(1 - n_{i,-\sigma}) + n_{i,-\sigma}\right) \qquad \sigma = \uparrow, \downarrow \tag{2.8}$$

and their Hermitean conjugates $Q_\sigma^\dagger$ satisfying commutation relations

$$\left\{Q_\uparrow, Q_\downarrow\right\} = 0 \qquad Q_\sigma^2 = 0 \qquad [\mathcal{H}, Q_\sigma] = (\mu - 2t_0 + \sigma h)Q_\sigma. \tag{2.9}$$

Fixing the potentials to $\mu = 2t_0$, $h = 0$ one obtains the supersymmetric model of [10] (up to the unitary transformation $T_1 T_2$).

It is important to identify the full symmetry of the model since it is well known that the Bethe ansatz states are all highest-weight states in this algebra and, hence, not complete [13], i.e. $S^+|\Psi_{\text{Bethe}}\rangle = 0 = Q_\sigma|\Psi_{\text{Bethe}}\rangle$. Only after complementing the Bethe ansatz states with those obtained by successive application of $S^{\pm}$ and $Q^{\dagger}_{\sigma}$ can the complete set of eigenfunctions be found. We shall come back to this question in the appendix. Note that as a consequence of (2.9) the number of particles in the states belonging to one $gl(2|1)$ multiplet range from the number $N_{\rm BA}$ in the Bethe ansatz state to $N_{\rm BA}+2$. Hence, in the thermodynamic limit investigated below particle densities $0 \leqslant n_{\rm e} < 2$ can be studied directly.

3. Bethe ansatz solution in the thermodynamic limit

Despite the derivation of Hamiltonian (1.1) in the framework of the quantum inverse scattering method, the spectrum of the model (which is obtainable in principle by means of the algebraic Bethe ansatz) has not been found in [10]. The difficulty here is the complicated representation theory for the superalgebra $gl(2|1)$.

In [14] the algebraic Bethe ansatz for lattice models with underlying q-deformed superalgebra $U_q(osp(2|2))$ (reducing to the model studied here in the rational $q \to 1$ limit) has been considered. Although the fusion procedure necessary to diagonalize the model works for special choices of the typical four-dimensional representations only, a conjecture is given for the general case.

On the other hand, it is straightforward to determine the spectrum using the *coordinate* Bethe ansatz: for models possessing internal symmetries, like the one considered here, the Schrödinger equation is solved with the ansatz [15]

$$\Psi(X_Q) = \sum_P A_{\sigma_1,\ldots,\sigma_N}(P|Q) \exp\left\{ \mathrm{i} \sum_{j=1}^{N} k_{p_j} x_j \right\} \tag{3.1}$$

where $Q = \{q_1, \ldots, q_N\}$ and $P = \{p_1, \ldots, p_N\}$ are permutations of the integers $\{1, \ldots, N\}$ and Q is chosen such that $X_Q = \{x_{q_1} < x_{q_2} < \cdots < x_{q_N}\}$. The coefficients $A(P|Q)$ from regions other than X_Q are connected with each other by elements of the two-particle S-matrix

$$S(k_1, k_2) = \frac{\vartheta(k_1) - \vartheta(k_2) + \mathrm{i}cP_{12}}{\vartheta(k_1) - \vartheta(k_2) + \mathrm{i}c} \tag{3.2}$$

(P_{12} is a spin permutation operator). Here the charge rapidities ϑ_j are related to the single-particle quasi-momenta k_j by $\vartheta(k) = \frac{1}{2}\tan(k/2)$, and the dependence on the system parameters (1.2) is incorporated in the parameter $c = (t_0 - t_2)/t_2$ (varying in the intervals $-1 < c < 0$ and $0 < c < \infty$). The $A(P|Q)$ are determined in a second Bethe ansatz for an inhomogeneous six-vertex model resulting in the Bethe ansatz equations (BAE)

$$\begin{aligned} \left(\frac{\vartheta_j - \mathrm{i}/2}{\vartheta_j + \mathrm{i}/2}\right)^L &= \prod_{\alpha=1}^{M} \frac{\vartheta_j - \lambda_\alpha + \mathrm{i}c/2}{\vartheta_j - \lambda_\alpha - \mathrm{i}c/2} \qquad j = 1, \ldots, N_{\rm e} \\ \prod_{j=1}^{N_{\rm e}} \frac{\lambda_\alpha - \vartheta_j + \mathrm{i}c/2}{\lambda_\alpha - \vartheta_j - \mathrm{i}c/2} &= -\prod_{\beta=1}^{M} \frac{\lambda_\alpha - \lambda_\beta + \mathrm{i}c}{\lambda_\alpha - \lambda_\beta - \mathrm{i}c} \qquad \alpha = 1, \ldots, M. \end{aligned} \tag{3.3}$$

The length L of the system is assumed to be even and $N_{\rm e}$ and M are the numbers of electrons and spin-$\downarrow$ electrons, respectively. Given a solution of (3.3) the eigenvalue of (1.1) in the corresponding state is

$$E = (2t_0 - \mu)N_{\rm e} - h\left(\frac{N_{\rm e}}{2} - M\right) - t_0 \sum_{j=1}^{N_{\rm e}} \frac{1}{\vartheta_j^2 + \frac{1}{4}}. \tag{3.4}$$

Comparing equations (3.3) and (3.4) with the spectrum conjectured in equations (71), (72) and (75) of [14] for $q \to 1$ we find that they do indeed coincide up to the normalization of the energies if one identifies $c = 1/(b - \frac{1}{2})$ (b being the continuous label of the typical four-dimensional $osp(2|2)$ representation $[b, \frac{1}{2}]$).

Solving (3.3), one has to distinguish the two different regions $c > 0$ and $c < 0$ as the character of the $\vartheta - \lambda$ solutions in these two cases is completely different. Note that the sign of the on-site Coulomb coupling U is the same as that of c because of (1.2). Hence the situation is very similar to the Hubbard model. We introduce some functions and their Fourier transforms that will be used in the following ($y > 0$):

$$\begin{aligned} a_y(x) &= \frac{1}{2\pi}\int_{-\infty}^{\infty} \mathrm{d}k\, \mathrm{e}^{-\mathrm{i}kx}\mathrm{e}^{-y|k|/2} = \frac{1}{2\pi}\frac{y}{x^2+y^2/4} \\ s_y(x) &= \frac{1}{2\pi}\int_{-\infty}^{\infty} \mathrm{d}k\, \mathrm{e}^{-\mathrm{i}kx}\frac{1}{2\cosh(yk/2)} = \frac{1}{2y\cosh(\pi x/y)} \\ R_y(x) &= (a_y * s_y)(x) = \frac{1}{2\pi y}\mathrm{Re}\left(\psi\left(1+\mathrm{i}\frac{x}{2y}\right) - \psi\left(\frac{1}{2}+\mathrm{i}\frac{x}{2y}\right)\right) \end{aligned} \tag{3.5}$$

where $(a*b)(x) = \int \mathrm{d}z\, a(x-z)b(z)$ denotes a convolution and ψ is the digamma function.

3.1. Repulsive case ($c > 0$)

In this case the solutions of (3.3) consist of real ϑ_j while the spin rapidities are known to be arranged in bound states of uniformly spaced sets of complex λ_α, the so called *n-strings*:

$$\lambda_\alpha^{n,j} = \lambda_\alpha^n + \mathrm{i}(n+1-2j)c/2 \qquad j = 1, 2, \ldots, n. \tag{3.6}$$

In the thermodynamic limit ($L \to \infty$ with particle density N_e/L and magnetization M/L being fixed) the solutions of the BAE (3.3) can be described in terms of densities $\rho(\vartheta)$ for charge rapidities and $\rho_h(\vartheta)$ for the corresponding holes. Similarly, one introduces density distributions σ_n ($\sigma_{n,h}$) for the n-strings of spin rapidities (and corresponding holes). Using standard procedures one obtains the following system of coupled linear integral equations from the BAE (3.3):

$$\begin{aligned} &\rho + \rho_h = a_1 + R_c * \rho - s_c * \sigma_{1,h} \\ &\sigma_1 + \sigma_{1,h} = s_c * (\sigma_{2,h} + \rho) \\ &\sigma_n + \sigma_{n,h} = s_c * (\sigma_{n+1,h} + \sigma_{n-1,h}) \qquad n \geqslant 2 \end{aligned} \tag{3.7}$$

The intervals in which the densities are non-vanishing depend on the state considered. The particle density and magnetization are related to ρ and σ_n through

$$\begin{aligned} n_e &= \frac{N_e}{L} = \int_{-\infty}^{\infty} \mathrm{d}\vartheta\, \rho(\vartheta) \\ m_z &= \frac{1}{L}\left(\frac{N_e}{2} - M\right) = \frac{n_e}{2} - \sum_{n=1}^{\infty}\int_{-\infty}^{\infty} \mathrm{d}\lambda\, n\sigma_n(\lambda). \end{aligned}$$

The energy density follows from (3.4):

$$e = \frac{E}{L} = (2t_0 - \mu)n_e - hm_z - 2\pi t_0 \int_{-\infty}^{\infty} \mathrm{d}\vartheta\, a_1(\vartheta)\rho(\vartheta). \tag{3.8}$$

The equilibrium distribution functions ρ and σ_n have to be determined by minimization of the free-energy functional, $\mathcal{F} = E - TS$, with the combinatorical entropy S of a particle and hole densities $\delta(\lambda)$ and $\delta_h(\lambda)$ given by [16]

$$\frac{S_\delta}{L} = \int_{-\infty}^{\infty} \mathrm{d}\lambda\, \{(\delta+\delta_h)\ln(\delta+\delta_h) - \delta\ln(\delta) - \delta_h\ln(\delta_h)\}. \tag{3.9}$$

Introducing the functions

$$\varepsilon_c(\vartheta) = T\ln\left(\frac{\rho_h}{\rho}\right) \qquad \varepsilon_n(\lambda) = T\ln\left(\frac{\sigma_{n,h}}{\sigma_n}\right) \tag{3.10}$$

and considering ρ and $\sigma_{n,h}$ as independent functions we obtain by variation of $\mathcal{F}$ the following nonlinear integral equations for the functions ε_α:

$$\begin{aligned}\varepsilon_c &= 2t_0 - \mu - 2\pi t_0 a_1 + Ts_c * \ln(n(\varepsilon_1)) + TR_c * \ln(n(-\varepsilon_c))\\ \varepsilon_1 &= -Ts_c * \ln(n(\varepsilon_2)) + Ts_c * \ln(n(-\varepsilon_c))\\ \varepsilon_n &= -Ts_c * (\ln(n(\varepsilon_{n+1})) + \ln(n(\varepsilon_{n-1}))) \qquad n \geqslant 2\end{aligned} \tag{3.11}$$

with the distribution function

$$n(\varepsilon) = (1 + \mathrm{e}^{\varepsilon/T})^{-1}. \tag{3.12}$$

Equations (3.11) have to be solved with the asymptotic boundary condition

$$\lim_{n\to\infty} \frac{\varepsilon_n}{n} = h. \tag{3.13}$$

The free-energy density is given by

$$f = T\int_{-\infty}^{\infty} \mathrm{d}\vartheta\, a_1(\vartheta)\ln(n(-\varepsilon_c(\vartheta))). \tag{3.14}$$

This shows that the functions ε_α are to be identified as renormalized ('dressed') energies of the single-particle excitations in the system.

3.2. *Attractive case* $(-1 < c < 0)$

In this regime one has—in addition to the real charge rapidities and strings of spin rapidities considered in the repulsive case—pairs of complex conjugated $\vartheta_j^\pm$ coupled to a real λ_j as solutions of the BAE (3.3):

$$\vartheta_j^\pm = \lambda_j' \pm \frac{\mathrm{i}|c|}{2}. \tag{3.15}$$

Note that for $c \to -1$, equation (3.3) would coincide with the BAE of the t–J model obtained in [3]; however, this value is out of the range accessible for this model. Following the same procedure as in the repulsive case we obtain in the thermodynamic limit

$$\begin{aligned}\rho + \rho_h &= s_{|c|} * \sigma_h' + s_{|c|} * \sigma_{1,h}\\ \sigma' + \sigma_h' &= a_{1-|c|} + R_{|c|} * \sigma_h' - s_{|c|} * \rho\\ \sigma_1 + \sigma_{1,h} &= s_{|c|} * (\sigma_{2,h} + \rho)\\ \sigma_n + \sigma_{n,h} &= s_{|c|} * (\sigma_{n+1,h} + \sigma_{n-1,h}) \qquad n \geqslant 2\end{aligned} \tag{3.16}$$

where $\sigma'(\lambda)$ and $\sigma_h'(\lambda)$ are the distribution functions for the paired rapidities (3.15) and corresponding holes.

Particle density and magnetization of the state corresponding to a solution of (3.16) are given by

$$\begin{aligned}n_e &= \int_{-\infty}^{\infty} \mathrm{d}\vartheta\, \rho(\vartheta) + 2\int_{-\infty}^{\infty} \mathrm{d}\lambda\, \sigma'(\lambda)\\ m_z &= \frac{1}{2}\int_{-\infty}^{\infty} \mathrm{d}\vartheta\, \rho(\vartheta) - \sum_{n=1}^{\infty}\int_{-\infty}^{\infty} \mathrm{d}\lambda\, n\sigma_n(\lambda)\end{aligned}$$

and the energy density is

$$e = (2t_0 - \mu)n_e - hm_z - 2\pi t_0 \int_{-\infty}^{\infty} d\vartheta\, a_1(\vartheta)\rho(\vartheta) - 2\pi t_0 \int_{-\infty}^{\infty} d\lambda\, (a_{1+|c|} + a_{1-|c|})(\lambda)\sigma'(\lambda). \tag{3.17}$$

Minimizing the free energy (with σ'_h as an additional independent function) and defining the dressed energy of the paired rapidities as

$$\varepsilon_p(\lambda) = T \ln\left(\frac{\sigma'_h}{\sigma}\right) \tag{3.18}$$

we obtain the thermodynamic BAE for the attractive case:

$$\begin{aligned}
\varepsilon_c &= Ts_{|c|} * \ln(n(\varepsilon_1)) - Ts_{|c|} * \ln(n(\varepsilon_p)) \\
\varepsilon_p &= 4t_0 - 2\mu - 2\pi t_0(a_{1+|c|} + a_{1-|c|}) - T(a_{2|c|} * \ln(n(-\varepsilon_p)) + a_{|c|} * \ln(n(-\varepsilon_c))) \\
\varepsilon_1 &= -Ts_{|c|} * (\ln(n(\varepsilon_2)) + \ln(n(-\varepsilon_c))) \\
\varepsilon_n &= -Ts_{|c|} * (\ln(n(\varepsilon_{n+1})) + \ln(n(\varepsilon_{n-1}))) \qquad n \geqslant 2
\end{aligned} \tag{3.19}$$

to be solved with the field boundary condition (3.13). The free-energy density is given by

$$f = T \int_{-\infty}^{\infty} d\vartheta\, (a_1(\vartheta) \ln(n(-\varepsilon_c)) + (a_{1-|c|} + a_{1+|c|}) \ln(n(-\varepsilon_p))). \tag{3.20}$$

4. Ground state and excitations at $T = 0$

We now want to examine properties of the zero-temperature ground state for the two cases. In this limit the distribution function n (3.12) in the thermodynamic BAE reduces to

$$\lim_{T\to 0} T \ln(n(\delta)) = -\delta^+ \tag{4.1}$$

where $\delta^+ > 0$ and $\delta^- < 0$ are the positive and negative parts of the function $\delta = \delta^+ + \delta^-$, respectively. At the same time it is clear that the ground-state configuration corresponds to the filling of all states with negative dressed energy ε_α.

4.1. Repulsive case ($c > 0$)

From (3.11) we find that $\varepsilon_{n>1}(\lambda) > 0$ for all λ. Using the asymptotic condition (3.13) we obtain from (3.11) with (4.1)

$$\begin{pmatrix} \varepsilon_c \\ \varepsilon_1 \end{pmatrix} = \begin{pmatrix} 2t_0 - \mu - 2\pi t_0 a_1 - h/2 \\ h \end{pmatrix} + \begin{pmatrix} 0 & a_c \\ a_c & -a_{2c} \end{pmatrix} * \begin{pmatrix} \varepsilon_c^- \\ \varepsilon_1^- \end{pmatrix}. \tag{4.2}$$

As in [17] one can prove that $\varepsilon_c(\vartheta)$ and $\varepsilon_1(\lambda)$ are monotonically increasing functions of $|\vartheta|$ and $|\lambda|$ and, consequently, they are negative in the intervals $[-Q, Q]$ and $[-B, B]$. For $h = 0$ two possible ground-state configurations are to be considered: the ferromagnetic state ($M = 0$ for $n_e \leqslant 1$ and $M = N_e - L$ for $n_e > 1$) and the antiferromagnetic state ($M = N_e/2$). The energy of the ferromagnetic state at fixed density n_e is simply

$$e_{\mathrm{FM}} = -2t_0 \begin{cases} \dfrac{1}{\pi} \sin \pi n_e & \text{for } n_e \leqslant 1 \\[2ex] \dfrac{1}{1+c}\left(\dfrac{1}{\pi} \sin \pi n_e - c(n_e - 1)\right) & \text{for } n_e > 1. \end{cases} \tag{4.3}$$

For the antiferromagnetic state one obtains from (3.7) that it corresponds to a filled band of one-strings, i.e. $B = \infty$. Hence σ_1 can be eliminated by Fourier transform and (3.7) simplifies to

$$\rho(\vartheta) = a_1(\vartheta) + \int_{-Q}^{Q} d\vartheta' \, R_c(\vartheta - \vartheta')\rho(\vartheta'). \tag{4.4}$$

Varying Q one obtains any filling between $n_e = 0$ and $n_e = 2$. For small Q, (4.4) can be solved by iteration and for $Q \to \infty$ by using Wiener–Hopf techniques [18] with the result

$$n_e = \begin{cases} \dfrac{4Q}{\pi} + 8\dfrac{\ln 2}{\pi^2 c}Q^2 + O(Q^3) & \text{for } Q \to 0 \\ 2 - \dfrac{2(c+1)}{\pi Q}\left(1 + c\dfrac{\ln(Q)}{2\pi Q}\right) + O\left(\dfrac{1}{Q^2}\right) & \text{for } Q \to \infty. \end{cases} \tag{4.5}$$

In the low-density limit we find that the ground state of the system is indeed antiferromagnetic. The energy difference to (4.3) is

$$e_{\mathrm{FM}} - e_0 = \begin{cases} \dfrac{\pi^2 \ln 2}{3c} n_e^4 + O(n_e^5) & \text{for } n_e \to 0 \\ \dfrac{4t_0}{1+c}(2 - n_e) + o\left((2-n_e)^2\right) & \text{for } n_e \to 2. \end{cases} \tag{4.6}$$

In figure 2 we present numerical data for the dependence of the (antiferromagnetic) ground-state energy of the system as compared to the ferromagnetic case for various values of the parameter c†.

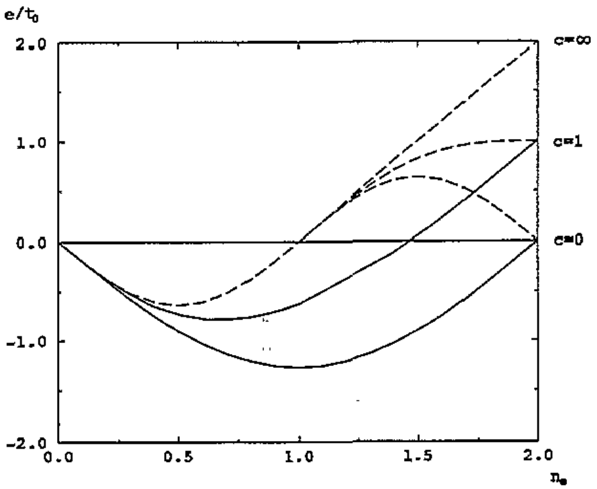

Figure 2. Energy of the antiferromagnetic ground state of the system (1.1) plotted against electron density in the repulsive regime for various values of the reduced coupling constant c. For comparison, the energy of the ferromagnetic state (4.3) is also included. Note, that for $c \to \infty$ the ferro and antiferromagnetic states are degenerate.

In the free-fermion limit $c \to 0$, (4.4) simplifies to

$$\rho(\vartheta) = a_1(\vartheta) + \frac{1}{2}\int_{-Q}^{Q} d\vartheta' \, \delta(\vartheta - \vartheta')\rho(\vartheta') \tag{4.7}$$

† In [12] the ground state is claimed to be *ferro*magnetic in this regime for densities $n_e < 1$. As is clear from equation (4.6), this is not correct.

and the ground-state energy is the expected result for this system

$$e_0 = -\frac{4t_0}{\pi}\sin\left(\frac{\pi n_e}{2}\right). \tag{4.8}$$

In the strong coupling limit $c \to \infty$ corresponding to $t_1 = t_2 = 0$, $t_3 = -t_0$, $U = 2t_0$, the ground state is degenerate with the ferromagnetic state (4.3).

There are two types of excitation that are to be considered in the low-energy sector: first, there are objects carrying charge ('holons') corresponding to particle- or hole-like excitations in the ground-state configuration of charge rapidities with energy $|\varepsilon(\vartheta)|$. Furthermore, there are spin-carrying objects ('spinons') corresponding to holes in the distribution of real spin rapidities. From (4.2) their energy is found to be

$$\varepsilon_1(\lambda) = \frac{1}{2c}\int_{-Q}^{Q} \mathrm{d}\vartheta\, \frac{|\varepsilon_c(\vartheta)|}{\cosh\frac{\pi}{c}(\lambda-\vartheta)}. \tag{4.9}$$

The physical excitations (for even particle number N_e) are even numbers of these objects forming a continuum of spin waves without gap. The energies of the spin rapidity strings of length $n > 1$ vanish.

Increasing the magnetic field the magnetization grows until it reaches its saturation value $\frac{1}{2}$ at the critical field h_c. For $h = h_c$ the interval for the λ integration vanishes, i.e. $B = 0$ (corresponding to $\varepsilon_1(\lambda = 0) = 0$). For $0 \leqslant n_e \leqslant 1$ we find

$$h_c = \frac{8t_0}{\pi}\frac{c(4Q^2+1)\arctan(2Q) - (4Q^2+c^2)\arctan(2Q/c)}{(c^2-1)(4Q^2+1)} \tag{4.10}$$

with $Q = \frac{1}{2}\tan(\pi n_e/2)$. In the limiting cases considered above, this expression becomes

$$\lim_{Q\to 0} h_c = 0 \qquad \lim_{Q\to\infty} h_c = 4t_2 \qquad \lim_{c\to 0} h_c = 4t_0\sin^2\left(\frac{\pi n_e}{2}\right). \tag{4.11}$$

4.2. *Attractive case* $(-1 < c < 0)$

Due to (3.19) the dressed energies of the spin rapidities $\varepsilon_{n\geqslant 1}(\lambda)$ are always positive. Performing the limit $T \to 0$ in (3.19) with equations (4.1) and (3.13) we obtain

$$\begin{pmatrix}\varepsilon_p\\ \varepsilon_c\end{pmatrix} = \begin{pmatrix}4t_0 - 2\mu - 2\pi t_0(a_{1+|c|} + a_{1-|c|})\\ 2t_0 - \mu - 2\pi t_0 a_1 - h/2\end{pmatrix} - \begin{pmatrix}a_{2|c|} & a_{|c|}\\ a_{|c|} & 0\end{pmatrix} * \begin{pmatrix}\varepsilon_p^-\\ \varepsilon_c^-\end{pmatrix}. \tag{4.12}$$

As in the repulsive regime one can prove that $\varepsilon_c(\vartheta)$ and $\varepsilon_p(\lambda)$ are monotonically increasing functions of the modulus of their arguments; hence, they are negative in the regions $[-Q, Q]$ and $[-B, B]$. Again we find that the ground state of the system is antiferromagnetic for $h = 0$ (see figure 3). In this regime the ground-state configuration consists of paired rapidities only ($Q = 0$). Their density is obtained from (3.16) which simplifies to

$$\sigma'(\lambda) = a_{1-|c|}(\lambda) + a_{1+|c|}(\lambda) - \int_{-B}^{B} \mathrm{d}\mu\, a_{2|c|}(\lambda-\mu)\sigma'(\mu). \tag{4.13}$$

Again, this is the ground-state configuration for any filling $0 \leqslant n_e \leqslant 2$ since

$$n_e = \begin{cases} \dfrac{8B}{\pi}\dfrac{2}{1-c^2} + \mathrm{O}(B^2) & \text{for } B \to 0\\ 2 - \dfrac{2(1-|c|)}{\pi B}\left(1 - \dfrac{|c|\ln(B)}{2\pi B}\right) + \mathrm{O}\left(\dfrac{1}{B^2}\right) & \text{for } B \to \infty. \end{cases} \tag{4.14}$$

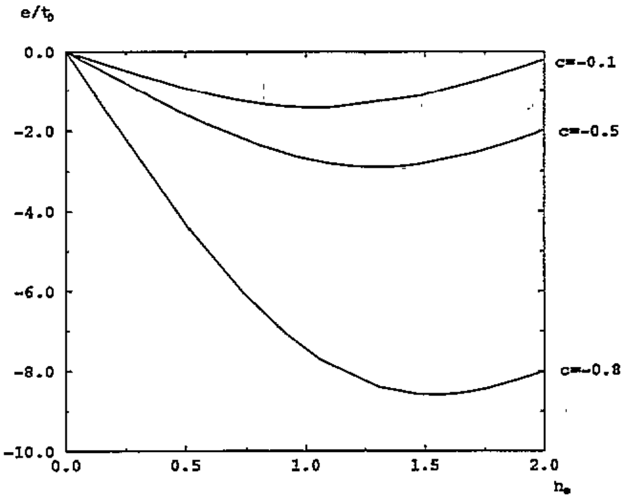

Figure 3. Energy of the antiferromagnetic ground state of the system (1.1) plotted against electron density in the attractive regime for various values of the reduced coupling constant c.

For $c \to 0$, (4.13) simplifies to

$$\sigma'(\lambda) = 2a_1(\lambda) - \int_{-B}^{B} \mathrm{d}\mu\, \delta(\lambda-\mu)\sigma'(\mu) \tag{4.15}$$

and we obtain for the ground-state energy (4.8) of the free-fermion system.

From equation (4.12) we obtain the dressed energy for excitations corresponding to real charge rapidities:

$$\varepsilon_c(\vartheta) = -\frac{h}{2} + \frac{1}{|c|}\int_B^{\infty} \mathrm{d}\lambda\, \frac{1}{\cosh((\vartheta-\lambda)\pi/c)}\varepsilon_p(\lambda). \tag{4.16}$$

Note that for vanishing magnetic field there is a gap $\Delta_c(n_e) = \varepsilon_c(0)$ for the creation of unpaired electrons. Δ_c is a monotonically falling function of n_e with its maximum at $\Delta_c(0) = 4t_0c^2/(1-c^2) > 0$ (see figure 4). The only massless excitations in this regime are charge-density waves corresponding to excitations within the band $\varepsilon_p(\lambda)$.

In an external magnetic field the nature of the excitations in the system change: for $h_{c1} = 2\Delta_c$ the gap for charge excitations closes and for h_{c2} the system undergoes a transition into the saturated ferromagnetic ground state. The latter corresponds to $B = 0$ (or, equivalently, $\varepsilon_p(0) = 0$). For $0 \leqslant n_e \leqslant 1$ we find

$$h_{c2} = \frac{8t_0c^2}{1-c^2} + \frac{8t_0}{\pi}\frac{(4B^2+c^2)\arctan(2B/|c|) - |c|(4B^2+1)\arctan(2B)}{(c^2-1)(4B^2+1)} \tag{4.17}$$

with $B = \frac{1}{2}\tan(\pi n_e/2)$. We obtain the limiting cases

$$\lim_{B\to\infty} h_{c2} = 4t_2 \qquad \lim_{B\to 0} h_{c2} = 2\Delta_c(0) \qquad \lim_{c\to 0} h_{c2} = 4t_0\sin^2\left(\frac{\pi n_e}{2}\right). \tag{4.18}$$

The non-vanishing of h_{c2} in the low density limit is a direct consequence of the gap of ε_c.

5. Finite size corrections and critical exponents

We now wish to study the finite size corrections of the spectrum in order to discuss the asymptotic behaviour of correlation functions. Again, the repulsive and the attractive case

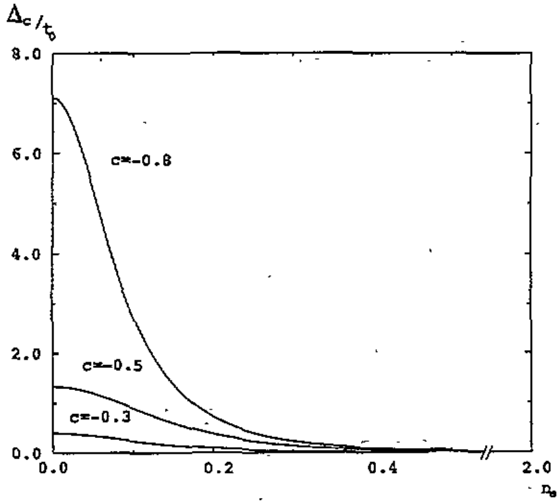

Figure 4. Energy gap for the creation of unpaired electrons as a function of the density of particles for several values of the parameter c.

are completely different and have to be treated separately.

5.1. Repulsive case ($c > 0$)

As found in section 4.1, for $T = 0$ the ground state and low-lying excitations are obtained from solutions of the BAE (3.3) with real ϑ's and λ's. Hence, we have the same situation as in the repulsive Hubbard model and following the procedure in [19] we obtain the finite size corrections of the ground-state energy as

$$E_0 - Le_0 = -\frac{\pi}{6L}(v_c + v_s) + o\left(\frac{1}{L}\right) \tag{5.1}$$

where v_c and v_s are the Fermi velocities of charge and spin density waves, respectively:

$$v_c = \frac{1}{2\pi\rho(Q)}\varepsilon_c'(Q) \qquad v_s = \frac{1}{2\pi\sigma_1(B)}\varepsilon_1'(B). \tag{5.2}$$

Similarly the energies and momenta of the low-lying excitations are given by

$$\begin{aligned} E(\Delta N, D) - Le_0 &= \frac{2\pi}{L}\left[v_c(\Delta_c^+ + \Delta_c^-) + v_s(\Delta_s^+ + \Delta_s^-)\right] + o\left(\frac{1}{L}\right) \\ P(\Delta N, D) - P_0 &= \frac{2\pi}{L}\left[\Delta_c^+ - \Delta_c^- + \Delta_s^+ - \Delta_s^-\right] + 2D_c\mathcal{P}_{F,\uparrow} + 2(D_c + D_s)\mathcal{P}_{F,\downarrow} \end{aligned} \tag{5.3}$$

with the conformal dimensions

$$\begin{aligned} 2\Delta_c^\pm(\Delta N, D) &= \left(Z_{cc}D_c + Z_{sc}D_s \pm \frac{Z_{ss}\Delta N_c - Z_{cs}\Delta N_s}{2\det(Z)}\right)^2 + 2N_c^\pm \\ 2\Delta_s^\pm(\Delta N, D) &= \left(Z_{cs}D_c + Z_{ss}D_s \pm \frac{Z_{cc}\Delta N_s - Z_{sc}\Delta N_c}{2\det(Z)}\right)^2 + 2N_s^\pm \end{aligned} \tag{5.4}$$

and the Fermi momenta $\mathcal{P}_{F,\uparrow(\downarrow)} = \frac{1}{2}\pi(n_e \pm 2m_z)$ of spin-up (down) electrons. The elements of the two-component vectors ΔN and D characterize the excited state: ΔN has integer components denoting the change of the number of electrons and down spins with respect to the ground state. D_c and D_s describe the deviations from the symmetric ground-state distributions. They are integers or half-odd integers depending on the parities of ΔN_c and ΔN_s:

$$D_c = \frac{\Delta N_c + \Delta N_s}{2} \bmod 1 \qquad D_s = \frac{\Delta N_c}{2} \bmod 1. \tag{5.5}$$

The matrix

$$Z = \begin{pmatrix} Z_{cc} & Z_{cs} \\ Z_{sc} & Z_{ss} \end{pmatrix} = \begin{pmatrix} \xi_{cc}(Q) & \xi_{sc}(Q) \\ \xi_{cs}(B) & \xi_{ss}(B) \end{pmatrix}^{\mathrm{T}} \tag{5.6}$$

parametrizing the conformal dimensions (5.4) is given in terms of the so called dressed charge matrix which satisfies a linear integral equation similar to (4.2) for the dressed energies:

$$\begin{pmatrix} \xi_{cc}(\vartheta) & \xi_{sc}(\vartheta) \\ \xi_{cs}(\lambda) & \xi_{ss}(\lambda) \end{pmatrix} = \begin{pmatrix} 1 & 0 \\ 0 & 1 \end{pmatrix} + \begin{pmatrix} 0 & a_c \\ a_c & -a_{2c} \end{pmatrix} * \begin{pmatrix} \xi_{cc}(\vartheta) & \xi_{sc}(\vartheta) \\ \xi_{cs}(\lambda) & \xi_{ss}(\lambda) \end{pmatrix}. \tag{5.7}$$

As shown above, the ground state at vanishing magnetic field corresponds to $B = \infty$ and with the aid of the Wiener–Hopf method [19] (5.6) simplifies to

$$Z = \begin{pmatrix} Z_{cc} & Z_{cs} \\ Z_{sc} & Z_{ss} \end{pmatrix} = \begin{pmatrix} \xi_c(Q) & 0 \\ \frac{1}{2}\xi_c(Q) & \sqrt{2}/2 \end{pmatrix} \tag{5.8}$$

where ξ_c is defined as the solution of the following scalar integral equation

$$\xi_c(\vartheta) = 1 + \int_{-Q}^{Q} \mathrm{d}\vartheta' \, R_c(\vartheta - \vartheta')\xi_c(\vartheta'). \tag{5.9}$$

As for the density, one can solve (5.9) near $Q = 0$ and $Q = \infty$ with the result

$$\xi_c(Q) = \begin{cases} 1 + \dfrac{2\ln 2}{\pi c} Q + \mathrm{O}(Q^2) & \text{for } Q \to 0 \\ \sqrt{2}\left(1 - \dfrac{c}{4\pi Q}\right) + \mathrm{o}\left(\dfrac{1}{Q}\right) & \text{for } Q \to \infty. \end{cases} \tag{5.10}$$

Hence the range of variation for the exponents determining the long distance asymptotics of the equal time correlators is the same as in the Hubbard and t–J models [20, 21]. Introducing $\theta = 2\xi_c^2(Q)$ the singularity of the momentum distribution function at the Fermi point is found to be

$$\begin{aligned} n_\sigma(k) &\sim \int \mathrm{d}x \, \mathrm{e}^{-\mathrm{i}kx} \langle c_{x,\sigma}(t = 0^+) c_{0,\sigma}(t = 0) \rangle \\ &\propto \mathrm{sgn}(k - \mathcal{P}_\mathrm{F})|k - \mathcal{P}_\mathrm{F}|^\nu \qquad \nu = \frac{1}{\theta} + \frac{\theta}{16} - \frac{1}{2} \end{aligned} \tag{5.11}$$

with a variation of the exponent ν in the interval $0 \leqslant \nu \leqslant \frac{1}{8}$ which shows the expected Luttinger liquid behaviour of this system.

Similarly, we obtain for the density–density and singlet-pair correlation functions $(\mathcal{P}_{\mathrm{F},\uparrow} = \mathcal{P}_{\mathrm{F},\downarrow} \equiv \mathcal{P}_\mathrm{F})$

$$\begin{aligned} G_{nn}(x) &= \langle (n_{x\uparrow} + n_{x\downarrow})(n_{0\uparrow} + n_{0\downarrow}) \rangle \\ &\sim n_\mathrm{e}^2 + A_1 \cos(2\mathcal{P}_\mathrm{F}x + \varphi_1) x^{-(1+\theta/4)} + A_2 \cos(4\mathcal{P}_\mathrm{F}x + \varphi_2) x^{-\theta} + A_3 x^{-2} \end{aligned} \tag{5.12}$$

$$G_p^{(0)}(x) = \langle c_{x+1,\uparrow}^\dagger c_{x,\downarrow}^\dagger c_{1,\downarrow} c_{0,\uparrow} \rangle \sim A \cos(2\mathcal{P}_\mathrm{F}x + \varphi) x^{-(4/\theta + \theta/4)}.$$

The leading order of the density–density correlator is given by the A_1 term with $3/2 < 1 + \theta/4 < 2$. Comparing this with the leading term of the singlet-pair correlator $5/2 > 4/\theta + \theta/4 > 2$ we see that density fluctuations are dominant.

In figure 5 we show lines of constant $\xi_c(Q)$ (hence identical critical behaviour) in the n_e–c parameter plane. Note that the strong coupling result $\xi_c(Q) = 1$ is found for less than half filling only. Beyond half filling the density dependence of the dressed charge is, for $c = \infty$,

$$\xi_c = \begin{cases} n_e & \text{for } n_e \to 1 \\ \sqrt{2}(1 - \frac{1}{8}(2 - n_e)) & \text{for } n_e \to 2. \end{cases} \tag{5.13}$$

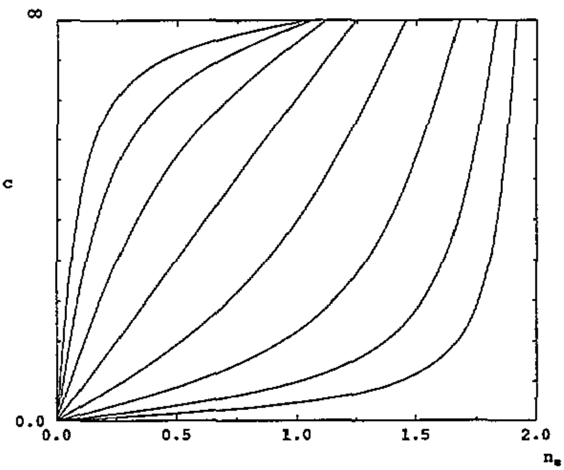

Figure 5. Contours of constant $\xi_c(Q)$ (and hence identical critical exponents) in the n_e–c parameter plane of the repulsive model. $\xi_c(Q)$ varies between 1 (at low densities) and $\sqrt{2}$ (the free fermionic case) for finite c.

As in [22] for the Hubbard model, this analysis of the critical behaviour can be extended to the case of magnetic fields. For small fields $h < h_c$ one has to expect logarithmic singularities in the exponents, while for fields $h > h_c$ the ground state is a saturated ferromagnetic one and spin density waves become massive giving a scalar dressed charge instead of (5.8).

5.2. *Attractive case $c > 0$*

As discussed in section 4.2 for $T = 0$ and $h < h_{c1}$ there is only one branch of massless excitations within the band ε_p†. The finite size corrections to the energies of the low-lying excitations are given by

$$E(\Delta N_p, D_p) - Le_0 = \frac{2\pi}{L} v_p(\Delta_p^+ + \Delta_p^-) + o\left(\frac{1}{L}\right)$$
$$P(\Delta N_p, D_p) - P_0 = \frac{2\pi}{L}(\Delta_p^+ - \Delta_p^-) + 2D_p\mathcal{P}_F \tag{5.14}$$

with

$$2\Delta_p^\pm(\Delta N_p, D_p) = \left(\xi_p(B)D_p \pm \frac{\Delta N_p}{2\xi_p(B)}\right)^2 + 2N_p^\pm \tag{5.15}$$

† In the analysis of the asymptotics of correlation functions for the model with $c = -1/2$ in [23] the existence of a second branch of massless excitations in the band of real charge rapidities ε_c is assumed. However, as shown in section 4.1 these have a gap for $h < h_{c1}$. Hence the results in [23] are incorrect.

and charge-density wave velocity $v_p = \varepsilon_p'(Q)/(2\pi\sigma'(Q))$. The dressed charge ξ_p is given by

$$\xi_p(\lambda) = 1 - \int_{-B}^{B} \mathrm{d}\lambda'\, a_{2|c|}(\lambda - \lambda')\xi_p(\lambda'). \tag{5.16}$$

With the same techniques as used above we obtain

$$\xi_p(B) = \begin{cases} 1 - \dfrac{2}{\pi|c|}B + \mathrm{O}(B^2) & \text{for } B \to 0 \\ \dfrac{\sqrt{2}}{2}\left(1 + \dfrac{|c|}{4\pi B}\right) + \mathrm{o}\left(\dfrac{1}{B}\right) & \text{for } B \to \infty. \end{cases} \tag{5.17}$$

The leading terms in the asymptotics of the equal time correlators as a function of $\theta = 2\xi_p^2(B)$ are the same as in the (attractive) Hubbard model [24]:

$$G_{nn}(x) \sim n_e^2 + A_1\frac{\cos(2\mathcal{P}_F x)}{x^\theta} + \frac{A_2}{x^2} \qquad G_p^{(0)}(x) \sim x^{-1/\theta}. \tag{5.18}$$

Comparing the leading exponents of these two correlators we see that the correlation of pairs ($1/2 \leqslant 1/\theta \leqslant 1$) overwhelms the density–density correlator ($2 \geqslant \theta \geqslant 1$) for arbitrary n_e. Hence, as in the attractive Hubbard model [24] we can conclude that the particles are confined in pairs which is reflected in the structure of the Bethe ansatz ground-state configuration.

In figure 6 we show lines in the n_e–$|c|$ parameter plane with identical critical behaviour.

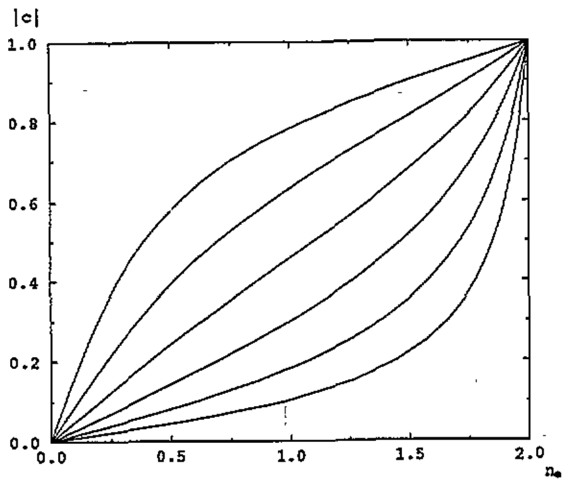

Figure 6. Contours of constant $\xi_p(Q)$ (and hence identical critical exponents) in the n_e–$|c|$ parameter plane of the attractive model at small magnetic fields $h < h_{c1}$. $\xi_p(Q)$ varies between 1 and $1/\sqrt{2}$ for any finite c.

For $h \geqslant h_{c1}$, charge and spin excitations are massless and the dressed charge is a 2×2 matrix as in the repulsive case. The same situation occurs in the attractive Hubbard model [24].

Acknowledgment

This work has been supported in part by the Deutsche Forschungsgemeinschaft under grant no Fr 737/2–1.

Appendix. Completeness of the Bethe ansatz states

As mentioned above, the Bethe ansatz states do not form the *complete* set of eigenstates of system (1.1) but are the highest-weight states of the $gl(2|1)$ superalgebra. Complementing the Bethe ansatz states with those obtained by the action of the $gl(2|1)$ shift operators one obtains additional eigenstates. The completeness of this *extended* Bethe ansatz has been proven (based on a string hypothesis (3.6) for the solutions of the BAE) for some models such as the the spin-$\frac{1}{2}$ Heisenberg chain, the supersymmetric t–J model and the Hubbard model [13, 25, 26]. In this appendix we present the study of the completeness for the two-site system together with some remarks on $L > 4$.

New eigenstates of the system are generated from the Bethe ansatz states by acting with the total spin operators S^-, S^+ and the supersymmetry generators Q_σ, $Q_\sigma^\dagger$. As a consequence of the anticommutativity of the latter (2.9) the resulting multiplet contains states in the N_e-, (N_e+1)- and (N_e+2)-particle sectors which are (we suppress the spin-multiplicity)

$$|\Psi_{\text{Bethe}}\rangle \xrightarrow{Q^\dagger_{\uparrow\downarrow}} \left\{ \begin{matrix} |\Psi_{Q1}\rangle \\ |\Psi_{Q2}\rangle \end{matrix} \right\} \xrightarrow{Q^\dagger_{\downarrow\uparrow}} |\Psi_{Q3}\rangle. \tag{A.1}$$

As shown above, the ground state of the model for a *fixed* number of particles is always a spin singlet. As a consequence of (.1) it is a member of a $gl(2|1)$ quartet, the same situation as in the related supersymmetric t–J model [25].

Solving the BAE (3.3) in the simplest case of the $L = 2$ system we obtain three *regular* Bethe ansatz states $|\psi_i\rangle$ with energy E_i (at the supersymmetric point $\mu = 2t_0$, $h = 0$):

$$\begin{aligned} &|\psi_1\rangle = |N_e = 0, M = 0\rangle \equiv |0\rangle \qquad E_1 = 0 \\ &|\psi_2\rangle = |N_e = 1, M = 0\rangle \equiv |k = 0, \uparrow\rangle \qquad E_2 = -4t_0 \\ &|\psi_3\rangle = |N_e = 2, M = 1\rangle \propto |\psi_{\uparrow\downarrow}\rangle - |\psi_{\downarrow\uparrow}\rangle + \frac{t_1}{t_0}(|\psi_{20}\rangle + |\psi_{02}\rangle) \qquad E_3 = -4(t_0 + t_2) \end{aligned} \tag{A.2}$$

with

$$|\psi_{\sigma_1\sigma_2}\rangle = c^\dagger_{1,\sigma_1} c^\dagger_{2,\sigma_2}|0\rangle \qquad |\psi_{20}\rangle = c^\dagger_{1,\uparrow} c^\dagger_{1,\downarrow}|0\rangle \qquad |\psi_{02}\rangle = c^\dagger_{2,\uparrow} c^\dagger_{2,\downarrow}|0\rangle. \tag{A.3}$$

Regular Bethe ansatz states are those corresponding to solutions of (3.3) with *finite* ϑ and λ [13, 26].

The one- and two-particle descendents of $|\psi_1\rangle$ are found to be the momentum π spin-doublet $|k = \pi, \sigma\rangle$ and the spin-singlet

$$|\psi_{\uparrow\downarrow}\rangle - |\psi_{\downarrow\uparrow}\rangle - \frac{t_0}{t_1}(|\psi_{20}\rangle + |\psi_{02}\rangle). \tag{A.4}$$

Analogously we find the descendents of $|\psi_2\rangle$ to be the following (degenerate) triplet and singlet states in the two-particle sector:

$$|\psi_{\uparrow\uparrow}\rangle \qquad |\psi_{02}\rangle - |\psi_{20}\rangle \tag{A.5}$$

and the doublet of zero-momentum single-hole states $|k_h = 0, \sigma\rangle$. Finally, $|\psi_3\rangle$ leads to the doublet of momentum π hole states $|k_h = \pi, \sigma\rangle$ and the completely filled state $|\psi_{22}\rangle$.

Hence the Bethe ansatz extended by means of the supersymmetry does indeed give the complete spectrum of states on the two-site lattice. Note that $|\psi_3\rangle$ is *always* the ground state of the two-particle sector for the range of parameters considered here. The difference between the repulsive and attractive regime is the larger amplitude of the states containing local pairs in the latter.

For general L, regular Bethe ansatz states will exist for particle numbers up to $2(L-1)$. Considering $L=4$ as an example one has to find 35 regular solutions of the BAE to generate a complete set of eigenstates. Four of these are states with $N_e > L$.

References

[1] Lieb E H and Wu F Y 1968 *Phys. Rev. Lett.* **20** 1445
[2] Sutherland B 1975 *Phys. Rev.* B **12** 3795
[3] Schlottmann P 1987 *Phys. Rev.* B **36** 5177
[4] Eßler F H L, Korepin V E and Schoutens K 1992 *Phys. Rev. Lett.* **68** 2960
[5] Bariev R Z, Klümper A, Schadschneider A and Zittartz J 1993 *J. Phys. A: Math. Gen.* **26** 1249
[6] Hirsch J E 1989 *Physica* **158C** 326
[7] Hirsch J E and Marsiglio F 1990 *Phys. Rev.* B **41** 2049
Marsiglio F and Hirsch J E 1990 *Phys. Rev.* B **41** 6435
[8] de Boer J, Korepin V E and Schadschneider A 1995 *Phys. Rev. Lett.* **74** 789
[9] Arrachea L and Aligia A A 1994 *Phys. Rev. Lett.* **73** 2240
[10] Bracken A J, Gould M D, Links J R and Zhang Y-Z 1995 *Phys. Rev. Lett.* **74** 2768
[11] Bedürftig G and Frahm H 1995 *Phys. Rev. Lett.* in press
[12] Karnaukhov I N 1994 *Phys. Rev. Lett.* **73** 1130
[13] Faddeev L D and Takhtajan L A 1984 *J. Sov. Math.* **24** 241; 1981 *Zap. Nauch. Semin. LOMI* **109** 134
[14] Maassarani Z 1995 *J. Phys. A: Math. Gen.* **28** 1305
[15] Yang C N 1967 *Phys. Rev. Lett.* **19** 1312
[16] Yang C N and Yang C P 1969 *J. Math. Phys.* **10** 1115
[17] Takahashi M 1972 *Prog. Theor. Phys.* **47** 69
[18] Yang C N and Yang C P 1966 *Phys. Rev.* **150** 327
[19] Woynarovich F 1989 *J. Phys. A: Math. Gen.* **22** 4243
[20] Frahm H and Korepin V E 1990 *Phys. Rev.* B **42** 10553
[21] Kawakami N and Yang S-K 1991 *J. Phys.: Condens. Matter* **3** 5983
[22] Frahm H and Korepin V E 1991 *Phys. Rev.* B **43** 5653
[23] Karnaukhov I N 1995 *Phys. Rev.* B **51** 7858
[24] Bogolyubov N M and Korepin V E 1990 *Theor. Math. Phys.* **82** 231
[25] Foerster A and Karowski M 1993 *Nucl. Phys.* B **396** 611
[26] Eßler F H L, Korepin V E and Schoutens K 1992 *Nucl. Phys.* B **384** 431